Improvement of Power System Stability Using HVDC Controls

P. Bapaiah

Abstract: In an AC/DC power system, emergency power actions from the HVDC connection are very important, because appropriate fast changes in DC power will reduce the stress on the AC system and the magnitude of the first transient swing. An HVDC transmission link is highly controllable. Its effective use depends on appropriate utilization of this controllability to ensure desired performance of the power system.

In this paper, the investigations are carried out on the improvement of power system stability by utilizing auxiliary controls for controlling HVDC power flow. AC/DC load flow using eliminated variable method is utilized in the transient stability analysis. Transient stability analysis is done on single machine system and multimachine system, using different control signals derived from the AC system. In this work, the combination of the different signals, which stabilizes the system, is found out and its effectiveness is verified.

Key words: HVDC controller, Multi machines, Stability, Power system, load modeling.

I. High-Voltage Direct-Current Transmission

Remote generation and system inter connections lead to a search for efficient power transmission at increasing power levels. The increase in voltage levels is not always feasible. The problems of AC transmission particularly in long distance transmission, has led to the development of DC transmission. However, as generation and utilization of power remains at alternating current, the DC transmission requires conversion at two ends, from AC to DC at the sending end and back to AC at the receiving end. This conversion is done at converter stations-rectifier at the sending end and inverter at the receiving end. The converters are static, using high power thyristors connected in series to give the required voltage ratings. The physical process of conversion is such that the same station can switch from rectifier to inverter by simple control action, thus facilitating the power reversal.

P. Bapaiah is currently working as an Assistant Professor in Electrical and Electronics Engineering Department at Amrita Sai Institute of Science and Technology, Paritala, (INDIA), Email: pagolubapaiah@gmail.com.

HVDC Transmission has advantages over AC transmission in special situations [1]. The following are the types of applications for which HVDC transmission has been used:

1. Under water cables longer than about 30 km. AC transmission is impractical for such distances because of the high capacitance of the cable requiring intermediate compensation stations.
2. Asynchronous link between two AC systems where AC ties would not be feasible because of system stability problems or a difference in nominal frequencies of the two systems.
3. Transmission of large amounts of power over long distances by over head lines. HVDC transmission is a competitive alternative to AC transmission for distances in excess of about 600 km.

Power System Stability

Power system stability is the ability of an electric power system, for a given initial operating condition, to regain a state of operating equilibrium after being subjected to a physical disturbance, with most system variables bounded so that practically the entire system remains intact [2].

The power system is a highly nonlinear system that operates in a constantly changing environment; loads, generator outputs and key operating parameters change continually. When subjected to a disturbance, the stability of the system depends on the initial operating condition as well as the nature of the disturbance. Stability of an electric power system is thus a property of the system motion around an equilibrium set, i.e., the initial operating condition. In an equilibrium set, the various opposing forces that exist in the system are equal instantaneously or over a cycle.

Power systems are subjected to a wide range of disturbances, small and large. Small disturbances in the form of load changes occur continually; the system must be able to adjust to the changing conditions and operate satisfactorily. It must also be able to survive numerous disturbances of a severe nature, such as a short circuit on a transmission line or loss of a large generator. A large disturbance may lead to structural changes due to the isolation of the faulted elements. At an equilibrium set, a power system may be stable for a given (large) physical disturbance, and unstable for another. It is impractical and uneconomical to design power systems to be stable for every possible disturbance [2]. The design contingencies are selected on the basis that they have a reasonably high probability of occurrence. Hence, large-disturbance stability always refers to a specified disturbance scenario.

The response of the power system to a disturbance may involve much of the equipment. For instance, a fault on a critical element followed by its isolation by protective relays will cause variations in power flows, network bus voltages, and machine rotor speeds; the voltage variations will actuate both generator and transmission network voltage regulators; the generator speed variations will actuate prime mover governors; and the voltage and frequency variations will affect the system loads to varying degrees depending on their individual characteristics. Further, devices used to protect individual equipment may respond to variations in system variables and cause tripping of the equipment, thereby weakening the system and possibly leading to system instability. If following a disturbance the power system is stable, it will reach a new equilibrium state with the system integrity preserved i.e., with practically all generators and loads connected through a single contiguous transmission system. Some generators and loads may be disconnected by the isolation of faulted elements or intentional tripping to preserve the continuity of operation of bulk of the system. Interconnected systems, for certain severe disturbances, may also be intentionally split into two or more "islands" to preserve as much of the generation and load as possible. The actions of automatic controls and possibly human operators will eventually restore the system to normal state. On the other hand, if the system is unstable, it will result in a run-away or run-down situation; for example, a progressive increase in angular separation of generator rotors, or a progressive decrease in bus voltages. An unstable system condition could lead to cascading outages and a shutdown of a major portion of the power system.

Power systems are continually experiencing fluctuations of small magnitudes. However, for assessing stability when subjected to a specified disturbance, it is usually valid to assume that the system is initially in a true steady-state operating condition.

Rotor angle stability refers to the ability of synchronous machines of an interconnected power system to remain in synchronism after being subjected to a disturbance. It depends on the ability to maintain/restore equilibrium between electromagnetic torque and mechanical torque of each synchronous machine in the system. Instability that may result occurs in the form of increasing angular swings of some generators leading to their loss of synchronism with other generators [2].

Loss of synchronism can occur between one machine and the rest of the system, or between groups of machines, with synchronism maintained within each group after separating from each other.

HVDC systems have the ability to rapidly control the transmitted power. Therefore, they have a significant impact on the stability of the associated AC power systems. An understanding of the characteristics of the HVDC systems is essential for the study of the stability of the power system. More importantly, proper design of the HVDC controls is essential to ensure satisfactory performance of the overall AC/DC system [1].

In this paper, an attempt is made to utilize the above advantage of HVDC systems for the improvement of stability of the power system.

II. AC/DC Load Flow

In transient stability studies it is prerequisite to do AC/DC load flow calculations in order to obtain system conditions prior to the disturbance. The simplest way of integrating a DC link into the AC load flow is representing it by constant active and reactive power injections at the two terminal buses in the AC systems. Thus the two terminal AC/DC buses are represented as a PQ-bus with a constant, voltage independent active and reactive power. However this is clearly an inadequate representation where the links contribution to AC system reactive power and voltage conditions is significant, since the accurate operating mode of the link and its terminal equipment are ignored [3].

Traditionally, two different approaches have been used to solve the power flow equations for hybrid AC/DC systems. The first approach is the sequential method, in which the AC and DC equations are solved separately in each iteration. The sequential method is easy to implement, but convergence problems may occur in certain situations. The other approach is the unified method, in which the solution vector is extended with the DC-variables, which can also be referred to as extended variable method. The drawback with the extended variable method is that it is complex to program and hard to combine with developments in AC power flow solution techniques.

The eliminated variable method used here [4] overcomes these difficulties. The basic idea is to treat the real and reactive powers consumed by the converters as voltage dependent loads. The DC equations are solved analytically or numerically and the DC variables are eliminated from the power flow equations. The method is unified, since the effect of the DC-link is included in the Jacobian. It is, however, not an extended variable method, since no DC variables are added to the solution vector.

DC System Model:

The equations describing the steady state behavior of a monopolar DC link can be summarized as follows.

$$V_{dr} = \frac{3\sqrt{2}}{\pi} a_r V_{tr} \cos\alpha_r - \frac{3}{\pi} X_c I_d \qquad (2.1)$$

$$V_{di} = \frac{3\sqrt{2}}{\pi} a_i V_{ti} \cos\gamma_i - \frac{3}{\pi} X_c I_d \qquad (2.2)$$

$$V_{dr} = V_{di} + r_d I_d \qquad (2.3)$$

$$P_{dr} = V_{dr} I_d \qquad (2.4)$$

$$P_{di} = V_{di} I_d \qquad (2.5)$$

$$S_{dr} = k \frac{3\sqrt{2}}{\pi} a_r V_{tr} I_d \qquad (2.6)$$

$$S_{di} = k\frac{3\sqrt{2}}{\pi} a_i V_{ti} I_d \tag{2.7}$$

$$Q_{dr} = \sqrt{S_{dr}^2 - P_{dr}^2} \tag{2.8}$$

$$Q_{di} = \sqrt{S_{di}^2 - P_{di}^2} \tag{2.9}$$

AC/DC Power Flow Equations:

When the DC-link is included in the power flow equations, only the mismatch equations at the converter terminal AC buses have to be modified.

$$\Delta P_{tr} = P_{tr}^{spec} - P_{tr}^{ac}(\delta, v) - P_{dr}(V_{tr}, V_{ti}, x_{dc}) \tag{2.10}$$

$$\Delta P_{ti} = P_{ti}^{spec} - P_{ti}^{ac}(\delta, v) + P_{di}(V_{tr}, V_{ti}, x_{dc}) \tag{2.11}$$

$$\Delta Q_{tr} = Q_{tr}^{spec} - Q_{tr}^{ac}(\delta, v) - Q_{dr}(V_{tr}, V_{ti}, x_{dc}) \tag{2.12}$$

$$\Delta Q_{ti} = Q_{ti}^{spec} - Q_{ti}^{ac}(\delta, v) - Q_{di}(V_{tr}, V_{ti}, x_{dc}) \tag{2.13}$$

where x_{dc} is a vector of internal DC-variables. The DC-variables satisfy

$$R(V_{tr}, V_{ti}, x_{dc}) = 0 \tag{2.14}$$

where R is a set of equations given by (2.1)-(2.3) and four control specifications.

In the extended variable method, (2.15) is solved iteratively.

$$\begin{bmatrix} \Delta P \\ \Delta P_t \\ \Delta Q \\ \Delta Q_t \\ \Delta R \end{bmatrix} = \left[\begin{array}{cc|c} H & N & \begin{matrix}0\\A\end{matrix} \\ \hline J & L & \begin{matrix}0\\C\end{matrix} \\ \hline \begin{matrix}0 & 0\end{matrix} & \begin{matrix}0 & D\end{matrix} & E \end{array}\right] \begin{bmatrix} \Delta\delta \\ \Delta\delta_t \\ \Delta V / V \\ \Delta V_t / V_t \\ \Delta x_{dc} \end{bmatrix} \tag{2.15}$$

In the sequential method, (2.14) is solved after each iteration of (2.16).

$$\begin{bmatrix} \Delta P \\ \Delta Q \end{bmatrix} = \left[\begin{array}{c|c} H & N \\ \hline J & L \end{array}\right] \begin{bmatrix} \Delta\delta \\ \Delta V / V \end{bmatrix} \tag{2.16}$$

Control Modes:

Seven variables and three independent equations, (2.1)-(2.3), are introduced when a DC-link is included. Hence, four specifications have to be made in order to define a unique solution. The control modes used here are summarized in Table 2.1, it will suffice to illustrate the analytical elimination procedure.

Control mode A is the base case, which in the well known current margin control corresponds to one terminal controlling the voltage and the other the current, or equivalently the power. The control angles and the DC-voltage are specified, and the converter transformer tap positions are varied in order to meet these specifications. The other modes in Table 2.1 are obtained from mode A if variables hit their limits during the power flow computations, or if the time scale is such that the taps can be assumed to be fixed. The modes that are obtained when limits are encountered depend on the control strategy of the HVDC-scheme, and this must be accounted for in the computations. For modes B - D, a_r determines α_r and a_i determines the direct voltage, which normally is the case for current control in the rectifier. For modes E - G, a_r determines the direct voltage. Subscript '*I*' refers to constant current control.

Table 0.1: Control modes

Control Mode	Specified Variables			
A	α_r	γ_i	V_{di}	P_{di}
B	a_r	γ_i	V_{di}	P_{di}
C	α_r	γ_i	a_i	P_{di}
D	a_r	γ_i	a_i	P_{di}
E	α_r	γ_i	a_r	P_{di}
F	α_r	a_i	V_{di}	P_{di}
G	α_r	a_i	a_r	P_{di}
A_I	α_r	γ_i	V_{di}	I_d
B_I	a_r	γ_i	V_{di}	I_d
C_I	α_r	γ_i	a_i	I_d
D_I	a_r	γ_i	a_i	I_d
E_I	α_r	γ_i	a_r	I_d
F_I	α_r	a_i	V_{di}	I_d
G_I	α_r	a_i	a_r	I_d

The taps are assumed to be continuous variables. Discrete tap positions can be taken into account by first assuming continuous taps and subsequently fix the taps at appropriate values.

The Eliminated Variable Method:

In the eliminated variable method, the equations in (2.14) are, *in principle*, solved for x_{dc}.

$$x_{dc} = f(V_{tr}, V_{ti}) \tag{2.17}$$

The real and reactive powers consumed by the converters can then be written as functions of V_{tr} and V_{ti}.

$$\begin{aligned} P_{dr} &= P_{dr}(V_{tr}, V_{ti}, x_{dc}) \\ &= P_{dr}(V_{tr}, V_{ti}, f(V_{tr}, V_{ti})) \\ &= P_{dr}(V_{tr}, V_{ti}) \end{aligned} \tag{2.18}$$

It is not needed to derive explicit functions for the real and reactive powers, only to find a sequence of computations such that the real and reactive powers and their partial derivatives w.r.t. the AC terminal voltages can be computed. If all real and reactive powers are written as functions of V_{tr} and V_{ti}, (2.15) can be replaced by (2.19).

$$\begin{bmatrix} \Delta P \\ \Delta Q \end{bmatrix} = \left[\begin{array}{c|c} H & N \\ \hline J & L \end{array}\right] \begin{bmatrix} \Delta\delta \\ \Delta V / V \end{bmatrix} \tag{2.19}$$

$$N'(tr,tr) = V_{tr}\frac{\partial P_{tr}^{ac}}{\partial V_{tr}} + V_{tr}\frac{\partial P_{dr}\left(V_{tr},V_{ti}\right)}{\partial V_{tr}} \quad (2.20)$$

$$N'(tr,ti) = V_{ti}\frac{\partial P_{tr}^{ac}}{\partial V_{ti}} + V_{ti}\frac{\partial P_{dr}\left(V_{tr},V_{ti}\right)}{\partial V_{ti}} \quad (2.21)$$

$$N'(ti,tr) = V_{tr}\frac{\partial P_{ti}^{ac}}{\partial V_{tr}} - V_{tr}\frac{\partial P_{di}\left(V_{tr},V_{ti}\right)}{\partial V_{tr}} \quad (2.22)$$

$$N'(ti,ti) = V_{ti}\frac{\partial P_{ti}^{ac}}{\partial V_{ti}} - V_{ti}\frac{\partial P_{di}\left(V_{tr},V_{ti}\right)}{\partial V_{ti}} \quad (2.23)$$

L' is modified analogously. Thus, in the eliminated variable method, four mismatch equations and up to eight elements of the Jacobian have to be modified, but *no new variables* are added to the solution vector, when a DC-link is included in the power flow. The partial derivatives are those required by (2.19); $\partial P_{dr}(V_{tr},V_{ti})/\partial V_{tr}$, for example, is the derivative of P_{dr} w.r.t. V_{tr}, assuming V_{ti} is kept constant. The DC variables, however, are not kept constant as opposed to $\partial P_{dr}(V_{tr},V_{ti},x_{dc})/\partial V_{tr}$, which is used in (2.15). Although (2.19) looks like (2.16), it is mathematically more similar to (2.15). The Jacobian in (2.19) is however normally more well-conditioned than the one in (2.15).

Analytical Elimination:

To illustrate the procedure, the analytical elimination is carried out in detail for some representative modes. It is sufficient to find P_d and S_d at each converter, since Q_d then can be computed with (2.8) or (2.9). The partial derivatives for all modes in Table2.1 are shown in Table 2.2 and Table 2.3.

Control Mode A:

$[\alpha_r \ \gamma_i \ V_{di} \ P_{di}]$

Since both the voltage and power at the inverter are specified, the direct current can be computed with (2.5), and P_{dr} can then be found by combining (2.3), (2.4) and (2.5)

$$P_{dr} = P_{di} + R_d I_d^2 \quad (2.24)$$

If we combine (2.l), (2.6) and (2.24), we obtain

$$S_{dr} = k\frac{P_{di} + \left(R_d + \frac{3}{\pi}X_c\right)I_d^2}{\cos\alpha_r} = k_\alpha\left(P_{di} + P_l + Q_l\right) \quad (2.25)$$

Analogously, for S_{di}:

$$S_{di} = \frac{k}{\cos\gamma_i}\left(P_{di} + Q_l\right) = k_\gamma\left(P_{di} + Q_l\right) \quad (2.26)$$

Thus, all real and reactive powers consumed by the converters can be precomputed, and including the dc-link in the power flow is trivial for this control mode. The same is true for any specification of the form $[\alpha_r \ \gamma_i \ x_1 \ x_2]$, where x_1 and x_2 are any two variables of $[P_{dr} \ P_{di} \ V_{dr} \ V_{di} \ I_d]$. The fact that the real and reactive powers can be precomputed for this case is well known.

Control Mode B:

$[\alpha_r \ \gamma_i \ V_{di} \ P_{di}]$

This mode occurs e.g. if the tap changer at the rectifier hits a limit in control mode A under current control in the rectifier. Since P_{di} and V_{di} are specified, I_d, V_{dr}, P_{dr} and S_{di} computed as for mode A. Since α_r is specified, S_{dr} is computed with (2.6) instead of (2.25).

$$V_{tr}\frac{\partial S_{dr}}{\partial V_{tr}} = V_{tr}\left(k\frac{3\sqrt{2}}{\pi}a_r I_d\right) = S_{dr} \quad (2.27)$$

$$V_{tr}\frac{\partial Q_{dr}}{\partial V_{tr}} = \frac{S_{dr}^2}{Q_{dr}} \quad (2.28)$$

The formulas for mode B_I are essentially identical; the only difference is that P_{di}, rather than I_d, is computed with (2.5). In general, when two of the variables of $[P_{dr} \ P_{di} \ V_{dr} \ V_{di} \ I_d]$ are specified, the other three can be computed from (2.3)-(2.5).

Control Mode C:

$[\alpha_r \ \gamma_i \ a_i \ P_{di}]$

These specifications are valid e.g. if the tap changer at the inverter hits a limit in mode A under current control in the rectifier. Combining (2.2) and (2.5) gives

$$P_{di} = \frac{3\sqrt{2}}{\pi}a_i V_{ti}\cos\gamma_i I_d - \frac{3}{\pi}X_c I_d^2 \quad (2.29)$$

If we solve for I_d, we obtain

$$I_d = c_1 V_{ti} - \sqrt{\left(c_1 V_{ti}\right)^2 - c_2 P_{di}} \quad (2.30)$$

$$\frac{\partial I_d}{\partial V_{ti}} = c_1 - \frac{c_1^2 V_{ti}}{\sqrt{\left(c_1 V_{ti}\right)^2 - c_2 P_{di}}} \quad (2.31)$$

where

$$c_1 = \frac{a_i\cos\gamma_i}{\sqrt{2}X_c} \quad (2.32)$$

$$c_2 = \frac{\pi}{3X_c} \quad (2.33)$$

Define ∂I_i as

$$\partial I_i = \frac{V_{ti}}{I_d}\frac{\partial I_d}{\partial V_{ti}} \quad (2.34)$$

Since P_{di} is specified, both its partials are zero. P_{dr} is given by (2.24), and its partial derivatives by:

$$V_{tr}\frac{\partial P_{dr}}{\partial V_{tr}} = 0 \quad (2.35)$$

$$V_{ti}\frac{\partial P_{dr}}{\partial V_{ti}} = 2R_d I_d^2\frac{V_{ti}}{I_d}\frac{\partial I_d}{\partial V_{ti}} = 2P_l\,\partial I_i \quad (2.36)$$

Since a_i is specified, S_{di} is computed with (2.7), and the partial derivatives of Q_{di} are given by

$$V_{tr}\frac{\partial Q_{di}}{\partial V_{tr}} = 0 \quad (2.37)$$

$$V_{ti}\frac{\partial Q_{di}}{\partial V_{ti}} = \frac{S_{di}^2}{Q_{di}}\left(1 + \partial I_i\right) \quad (2.38)$$

Q_{dr} and its partial derivatives are computed from (25)

$$V_{ti}\frac{\partial S_{dr}}{\partial V_{ti}} = 2\partial I_i k_\alpha \left(P_l + Q_l\right) \tag{2.39}$$

$$V_{tr}\frac{\partial Q_{dr}}{\partial V_{tr}} = 0 \tag{2.40}$$

$$V_{ti}\frac{\partial Q_{dr}}{\partial V_{ti}} = \frac{2\partial I_i}{Q_{dr}}\left[k_\alpha S_{dr}\left(Q_l + P_l\right) - P_l P_{dr}\right] \tag{2.41}$$

Other Modes

The partial derivatives for the other control modes can be derived analogously; if the tap changer controlling the control angle is specified (modes B, D, F, G), only the reactive power at that converter will depend on corresponding AC voltage.

If the tap changer controlling the direct voltage is specified (modes C, D, E, G), all the real and reactive powers will depend on the AC voltage at that terminal. Equations (2.30) or (2.43) are used to find the direct current for constant power control.

If the tap changer position is specified at a converter, S_d is computed with (2.6) or (2.7), otherwise (2.25) or (2.26) are used. The partial derivatives for all modes in Table 2.1 are summarized in Table 2.2 and Table 2.3

Table 0.2: Partial derivatives for modes with the direct voltage determined by a_i

Mode	$\frac{\partial P_{di}}{\partial V_{ti}}$	$V_{tr}\frac{\partial}{\partial}$	$V_{ti}\frac{\partial}{\partial}$	$V_{ti}\frac{\partial Q_{dr}}{\partial V_{ti}}$	$\frac{\partial P_{di}}{\partial V_{ti}}$	$\frac{\partial Q_{di}}{\partial V_{ti}}$	$V_{ti}\frac{\partial}{\partial}$	$V_{ti}\frac{\partial Q_{di}}{\partial V_{ti}}$
A	0	0	0	0	0	0	0	0
A_I	0	0	0	0	0	0	0	0
B	0	$\frac{S_{dr}^2}{Q_{dr}}$	0	0	0	0	0	0
B_I	0	$\frac{S_{dr}^2}{Q_{dr}}$	0	0	0	0	0	0
C	0	0	$2P_l\partial$	$\frac{2\partial I_i}{Q_{dr}}\left[k_\alpha S_{dr}\left($	0	0	0	$\frac{S_{di}^2}{Q_{di}}\left($
C_I	0	0	$P_{di}+$	$\frac{\left(P_{di}+Q_l\right)}{Q_{dr}}\left[k_\alpha S\right.$	0	0	$P_{di}+$	$Q_{di}-\frac{P}{Q}$
D	0	$\frac{S_{dr}^2}{Q_{dr}}$	$2P_l\partial$	$\frac{\partial I_i}{Q_{dr}}\left[S_{dr}^2 - 2P_l\right.$	0	0	0	$\frac{S_{di}^2}{Q_{di}}\left($
D_I	0	$\frac{S_{dr}^2}{Q_{dr}}$	$P_{di}+$	$-\frac{\left(P_{di}+Q_l\right)}{Q_{dr}}P_{dr}$	0	0	$P_{di}+$	$Q_{di}-\frac{P}{Q}$

Table 0.3: Partial derivatives for modes with the direct voltage determined by a_r

Mode	$V_{tr}\frac{\partial}{\partial}$	$V_{tr}\frac{\partial Q_{dr}}{\partial V_{tr}}$	$\frac{\partial P_{di}}{\partial V_{ti}}$	$\frac{\partial Q_{di}}{\partial V_{ti}}$	$V_{tr}\frac{\partial}{\partial}$	$V_{tr}\frac{\partial Q_{di}}{\partial V_{tr}}$	$\frac{\partial P_{di}}{\partial V_{ti}}$	$V_{ti}\frac{\partial}{\partial}$
E	$2P_l\partial$	$\frac{S_{dr}^2\left(1+\partial I_r\right.}{Q_{dr}}$	0	0	0	$\frac{2\partial I_r}{Q_{di}}Q_l k_\gamma$	0	0
E_I	$P_{dr}+$	$Q_{dr}-\frac{P_{dr}}{Q_{dr}}Q$	0	0	$P_{dr}+$	$\frac{P_{dr}+Q_l}{Q_{di}}\left[k\right.$	0	0
F	0	0	0	0	0	0	0	$\frac{S_{di}^2}{Q_{di}}$
F_I	0	0	0	0	0	0	0	$\frac{S_{di}^2}{Q_{di}}$
G	$2P_l\partial$	$\frac{S_{dr}^2\left(1+\partial I_r\right.}{Q_{dr}}$	0	0	0	$\frac{S_{di}^2}{Q_{di}}\partial I_r$	0	$\frac{S_{di}^2}{Q_{di}}$
G_I	$P_{dr}+$	$Q_{dr}-\frac{P_{dr}}{Q_{dr}}Q$	0	0	$P_{dr}+$	$-\frac{P_{dr}+Q_l}{Q_{di}}$	0	$\frac{S_{di}^2}{Q_{di}}$

∂I_r in Table 2.3 is defined as

$$\partial I_r = \frac{V_{tr}}{I_d}\frac{\partial I_d}{\partial V_{tr}} \tag{2.42}$$

where

$$I_d = c_3 V_{tr} - \sqrt{\left(c_3 V_{tr}\right)^2 - c_4 P_{di}} \tag{2.43}$$

$$c_3 = \frac{3a_r \cos\alpha_r}{\sqrt{2}\left(\pi R_d + 3X_c\right)} \tag{2.44}$$

$$c_4 = \frac{\pi}{\pi R_d + 3X_c} \tag{2.45}$$

A drawback with the analytical elimination is that the formulas have to be re-derived for other DC system configurations or if other specifications are used.

Transient Stability Studies:

Transient stability studies provide information related to the capability of a power system to remain in synchronism during major disturbances resulting from either the loss of generating or transmission facilities, sudden or sustained load changes, or momentary faults. Specifically, these studies provide the changes in the voltages, currents, powers, speeds, and torques of the machines of the power

system, as well as the changes in system voltages and power flows, during and immediately following a disturbance. The degree of stability of a power system is an important factor in the planning of new facilities. In order to provide the reliability required by the dependence on continuous electric service, it is necessary that power systems be designed to be stable under any conceivable disturbance.

The performance of the power system during the transient period can be obtained from the network performance equations. The performance equation using the bus frame of reference in either the impedance or admittance form has been used in transient stability calculations.

The operating characteristics of synchronous and induction machines are described by sets of differential equations. The number of differential equations required for a machine depends on the details needed to represent accurately the machine performance.

A transient stability analysis is performed by combining a solution of the algebraic equations describing the network with a numerical solution of the differential equations. The solution of the network equations retains the identity of the system and thereby provides access to system voltages and currents during the transient period [5].

As compared with rotor long-time constants, the AC and DC-transmission systems respond rapidly to network and load changes. The time constants associated with the network variables are extremely small and can be neglected without significant loss of accuracy. The synchronous machine stator time constants may also be taken as zero.

The DC link is assumed here to maintain normal operation throughout the disturbance. This approach is not valid for larger disturbances such as converter faults, DC-line faults and AC faults close to the converter stations, these disturbances can cause commutation failures and alter the normal conduction sequence [6].

III. SYSTEM REPRESENTATION

Generator Representation

The synchronous machine is represented by a voltage source, in back of a transient reactance, that is constant in magnitude but changes in angular position. This representation neglects the effect of saliency and assumes constant flux linkages and a small change in speed. If the machine rotor speed is assumed constant at synchronous speed, a normal and accepted assumption for stability studies, then M is constant. If the rotational power losses of the machine due to such effects as windage and friction are ignored, then the accelerating power equals the difference between the mechanical power and the electrical power [6]. The classical model can be described by the following set of differential and algebraic equations:
Differential:

$$\frac{d\delta}{dt} = \omega - 2\pi f$$

$$\frac{d^2\delta}{dt^2} = \frac{d\omega}{dt} = \frac{\pi f}{H}\left(P_m - P_e\right)$$

Algebraic:

$$E^{'} = E_t + r_a I_t + jx_d^{'} I_t$$

where E'=voltage back of transient reactance
E_t=machine terminal voltage
I_t=machine terminal current
r_a=armature resistance
$x_d^{'}$ =transient reactance

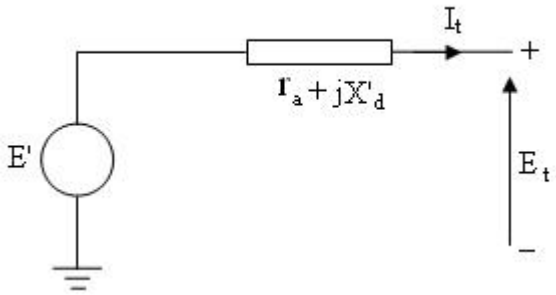

Figure 0.1: Generator Classical model

Representation of Loads

Power system loads, other than motors represented by equivalent circuits, can be treated in several ways during the transient period. The commonly used representations are either static impedance or admittance to ground, constant real and reactive power, or a combination of these representations. The parameters associated with static impedance and constant current representations are obtained from the scheduled bus loads and the bus voltages calculated from a load flow solution for the power system prior to a disturbance [5]. The initial value of the current for a constant current representation is obtained from

$$I_{po} = \frac{P_{lp} - jQ_{lp}}{E_p^*}$$

The static admittance Y_{po} used to represent the load at bus P, can be obtained from

$$Y_{po} = \frac{I_{po}}{E_p}$$

where E_p is the calculated bus voltage, P_{lp} and Q_{lp} are the scheduled bus loads. Diagonal elements of Admittance matrix (Y – Bus) corresponding to the load bus are modified using the Y_{po}.

Representation of HVDC Systems

Each DC system tends to have unique characteristics tailored to meet the specific needs of its application. Therefore, standard models of fixed structures have not been developed for representation of DC systems in stability studies [1].

a) Converter model

i) Simplified model

Here valve switching is neglected and the converter is represented by the average DC voltage equation. This model is similar to that used in power flow analysis. The transformer tap is assumed to be constant as the tap changer dynamics are very slow [7]. This model is inaccurate during severe disturbances. It cannot handle commutation failures and cannot predict the converter behavior during unsymmetrical faults.

ii) Detailed model

Here, the valve switching is incorporated and the model is free from the drawbacks associated with the simplified model. However the transient simulation of converter now requires integration step size as small as 50 – 100 μs. This implies heavy computation burden, so it is used only for short duration (say 0.2 sec) immediately after the disturbance.

b) Converter controller models

i) Response type model

The dynamics of the CEA and CC are neglected and only the steady – state controller characteristics are represented. The main feature of this type of controller model is that the configuration and the parameters of the controller are assumed to designed at a later stage basing on the requirement.

ii) Detailed representation

It requires the analysis of actual control circuitry and the establishment of a dynamic equivalent with a frequency response which matches the actual controller response. This is used along with the detailed converter model.

c) DC network model

i) Resistive network

Here DC network is represented as resistive network ignoring energy storage elements. This approach is valid when DC lines are short and or for back to back HVDC links and smoothing reactors are of moderate size.

ii) Transfer function representation

For a two terminal DC link with the response type controller, an alternative representation of the DC network is to use a transfer function (Fig. 2.2) instead of a resistance. In this case, the time constant T_{dc} represents the delay in establishing the DC current after a step change in the order is given.

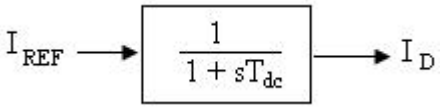

Figure 0.2: Transfer Function Model

iii) Dynamic representation

As the frequency bandwidth of the response model considered in the transient stability studies is modest, it is adequate to represent the dc network by a simple equivalent circuit of the type shown in figure no 2.3. Even here, the shunt branches may be neglected.

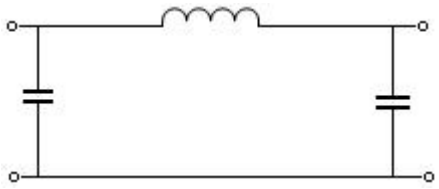

Figure 0.3: Equivalent Circuit

Runge-Kutta method

In the application of the Runge-Kutta fourth-order approximation, the changes in the internal voltage angles and machine speeds, again for the simplified machine representation, are determined from

$$\Delta\delta_{i(t+\Delta t)} = \frac{1}{6}\left(k_{1i} + 2k_{2i} + 2k_{3i} + k_{4i}\right)$$

$$\Delta\omega_{i(t+\Delta t)} = \frac{1}{6}\left(l_{1i} + 2l_{2i} + 2l_{3i} + l_{4i}\right)$$

i=1,2,…,no. of generators.

The k's and l's are the changes in δ_i and ω_i respectively, obtained using derivatives evaluated at predetermined points. For this procedure the network equations are to be solved four times.

Steps of the AC-DC Transient Stability Study

Generally, the DC scheme interconnects two or more, otherwise independent, AC systems and the stability assessment is carried out for each of them separately, taking into account the power constraints at the converter terminal. If the DC link is part of a single (synchronous) AC system, the converter constraints will apply to each of the nodes containing a converter terminal. The basic structure of transient stability program is given below [5]:

1) The initial bus voltages are obtained from the AC/DC load flow solution prior to the disturbance.
2) After the AC/DC load flow solution is obtained, the machine currents and voltages behind transient reactance are calculated.
3) The initial speed is equated to 2π f and the initial mechanical power is equated to the real power output of each machine prior to the disturbance.
4) The network data is modified for the new representation. Extra nodes are added to represent the generator internal voltages. Admittance matrix is modified to incorporate the load representation.
5) Set time, t=0;
6) If there is any switching operation or change in fault condition, modify network data accordingly and run the AC/DC load flow.
7) Using Runge-Kutta method, solve the machine differential equations to find the changes in the internal voltage angle and machine speeds.
8) Internal voltage angles and machine speeds are updated and are stored for plotting.
9) AC/DC load flow is run to get the new output powers of the machine.
10) Advance time, t=t+Δt.

11) Check for time limit, if t ≤ tmax repeat the process from step 6, else plot the graphs of internal voltage angle variations and stop the process.

Basing on the plots, that we get from the above procedure it can be decided whether the system is stable or unstable. In case of multi machine system stability analysis the plot of relative angles is done to evaluate the stability.

a. Basic Control Principles

The HVDC system is basically constant-current controlled for the following two important reasons:

- To limit overcurrent and minimize damage due to faults.
- To prevent the system from running down due to fluctuations of the ac voltages.

It is because of the high-speed constant current control characteristic that the HVDC system operation is very stable [1]. The following are the significant aspects of the basic control system:

a) The rectifier is provided with a current control and an α-limit control. The minimum α reference is set at about 5^0 so that sufficient positive voltage across the valve exists at the time of firing, to ensure successful commutation. In the current control mode, a closed loop regulator controls the firing angle and hence the dc voltage to maintain the direct current equal to the current order. Tap changer control of the converter transformer brings α with in the range of 10^0 to 20^0. A time delay is used to prevent unnecessary tap movements during excursions of α.

b) The inverter is provided with a constant extinction angle (CEA) control and current control. In the CEA control mode, γ is regulated to a value of about 15^0. This value represents a trade-off between acceptable var consumption and a low risk of commutation failure. Tap changer control is used to bring the value of γ close to the desired range of 15^0 to 20^0.

c) Under normal conditions, the rectifier is on current control mode and the inverter is on CEA control mode. If there is a reduction in the ac voltage at rectifier end, the rectifier firing angle decreases until it hits the α_{min} limit. At this point, the rectifier switches to α_{min} control and the inverter will assume current control.

d) To ensure satisfactory operation and equipment safety, several limits are recognized in establishing the current order: maximum current limit, minimum current limit, and voltage-dependent current limit.

e) Higher-level controls may be used, in addition to the above basic controls, to improve AC/DC system interaction and enhance AC system performance.

All schemes used to date have used the above modes of operation for the rectifier and the inverter. However, there are some situations that may warrant serious investigation of a control scheme in which the inverter is operated continuously in current control mode and the rectifier in α-minimum control mode. Enhanced performance into weak systems may be one case.

b. Controls for Enhancement of AC System Performance

In a DC transmission system, the basic controlled quantity is the direct current, controlled by the action of the rectifier with the direct voltage maintained by the inverter. A DC link controlled in this manner buffers one AC system from disturbances on the other. However, it does not allow the flow of synchronizing power which assists in maintaining stability of AC systems. The converters in effect appear to the AC systems as frequency-insensitive loads and this may contribute to negative damping of system swings [1]. Further, the DC links may contribute to voltage collapse during swings by drawing excessive reactive power.

Supplementary controls are therefore often required to exploit the controllability of DC links for enhancing the AC system dynamic performance. There are a variety of such higher level controls used in practice. Their performance objectives vary depending on the characteristics of the associated AC systems. The following are the major reasons for using supplementary control of DC links:

- Improvement of damping of AC system electromechanical oscillations.
- Improvement of transient stability.
- Isolation of system disturbance.
- Frequency control of small isolated systems.
- Reactive power regulation and dynamic voltage support.

The controls used tend to be unique to each system. To date, no attempt has been made to develop generalized control schemes applicable to all systems. The supplementary controls use signals derived from the AC systems to modulate the DC quantities. The modulating signals can be frequency, voltage magnitude and angle, and line flows. The particular choice depends on the system characteristics and the desired results.

In order to augment transient stability limit large signal modulation is used, thereby improving system security. Large changes in the power flow in the DC link are required to compensate for tripping of loads, generators or AC ties. While overload capability in DC links is useful, the limits imposed by ratings of the link usually do not curtail the benefits of power modulation. Hence, significant improvements can be expected out of the use of DC links in emergency control. The rapid response of DC link controllers makes it possible to arrest large fluctuations in the frequency by matching generation to the load in the area to which the DC link is connected [7]. It is desirable to obtain control signals locally. Some of the controls that can be used are as follows:

- Rotor frequency of adjacent generator
- Frequency at the converter bus
- Power or current in adjacent, parallel AC tie.

- Phase angle changes in the AC system [8].

The above signals work satisfactorily for the single machine system case. However, in the case of multimachine system it may be necessary to employ control signals derived from relative angle deviation, speed deviation and acceleration and different combinations of these signals. Apart from linear controllers, (like P, PI and PID controllers) Fuzzy logic controllers can also be employed which are known to give better performance. The output of Fuzzy Logic Controller is utilized to modulate the power order of the DC control, which in turn modulates the DC power.

The stabilizing control is implemented through large signal modulation of power in response to a control signal derived from the AC system variables. The effectiveness of the control can be enhanced by increased overload rating of the converters which permit short – term overloads. Thus, the rapid controllability of power in a DC link can be used to advantage in improving the transient stability of the AC system in which the DC link is embedded. The power flow can even be reversed in a short time (less than 0.25sec). Thus, DC link control can be viewed as an alternative to fast valving or braking resistor.

IV. Proposed Work

In this work, the advantage of fast HVDC power modulation is utilized to improve the stability of the system with different types of controllers and control signals.

i. Case 1

A single machine system is considered with parallel AC and DC transmission, having a Type – 0 Auxiliary controller and a Proportional Integral type current controller for the HVDC system. Here, the control signals are derived from generator speed deviation, generator phase angle deviation and variations of power in the parallel AC line are used and combinations of these signals are also utilized.

ii. Case 2

A multi machine system is considered with a HVDC link having a Proportional Integral current controller. The auxiliary controller is a constant gain controller which is given with different control signals from the AC system. The control signals are derived from relative generator angles, relative speed variations and accelerations of different generators.

iii. Auxiliary Stabilizing Controller

A Type- 0 controller is used here and is shown in figure 4.1. By this, we can get fast response by increasing the gain constant (Kw) or decreasing the time constant (Tw) [7]. The gain constant (Kw) varies from 0.0 to 1.0 and time constant varies from 0.01 to 0.1. These two constants depend on system size and magnitude of the disturbance. Similarly this type of auxiliary controller is tested for a single machine AC/DC system at different gain constants (Kw) and satisfactory results are obtained.

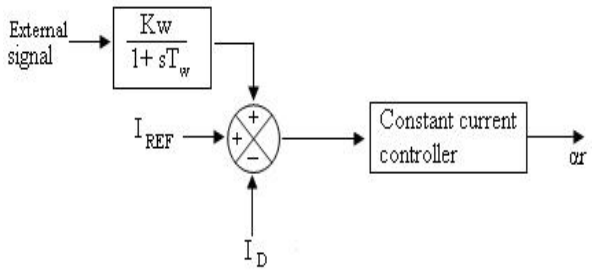

Figure 0.4: Type - 0 Controller

iv. Constant Current Controller

Here Proportional Integral (PI) type controller is used [7]. This type of controller has feedback signal (I_{DC}) to regulate the firing angle (Alfa) at the rectifier end to maintain the DC link current constant and the same is shown in figure 4.2.

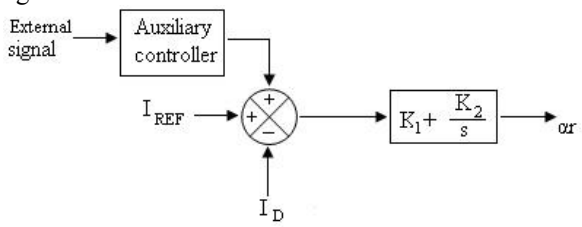

Figure 0.5: Constant Current Controller

v. Test System

A single machine system connected to infinite bus through parallel AC and DC links is considered and is shown in figure 4.3.

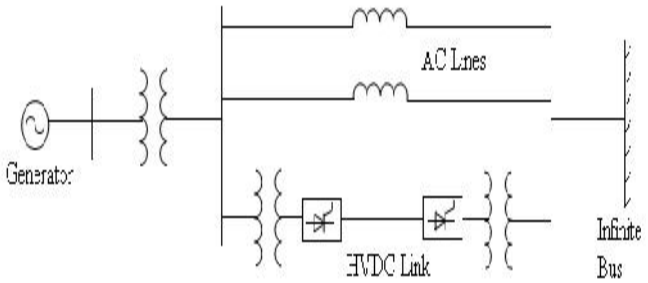

Figure 0.6: Parallel AC and DC system

The single machine system, using the Type – 0 auxiliary controller and a Proportional Integral type current controller for HVDC link is used to demonstrate the enhancement of stability by utilizing the controllability of the HVDC line. The DC link is represented by a simplified transfer function model. The following numerical data on 100 MVA base is used.

vi. System Data

- Generator :

  Pg=3.0 pu H=6.0 pu
  X_d=0.1 pu D=0.01
  F=50Hz

- AC transmission lines:

X_{eq} = 0.15 pu

- Transformer:
  X_t=0.05 pu
- DC link:
  K_1=0.4 K_2=0.3 T_w=0.05
  L_d=0.03 R_d=0.05 X_c=0.126
- Initial conditions
  δ=0.6435
  Δw =0
  I_d=0.8957
  Alfa=0.279
  V_{di}=0.99

The analysis is performed using the disturbances like variations in mechanical power (0.3 pu) and outage of one of the parallel AC lines. The stability of the system is enhanced utilizing different stabilizing signals for power modulation in the HVDC link.

vii. Case A: Mechanical Power Variations

The mechanical power of the generator is increased by 0.3 pu and different control signals from the AC system are utilized for the stability improvement. Without any external control signal applied to the HVDC system the stability analysis is performed and the generator angle plot is as shown in figure no. 4.4. Considering variations in speed and parallel AC tie power variations different control signals are applied to HVDC controller. The plots of phase angles of generator for different stabilizing signals are shown in figures 4.5 – 4.9.

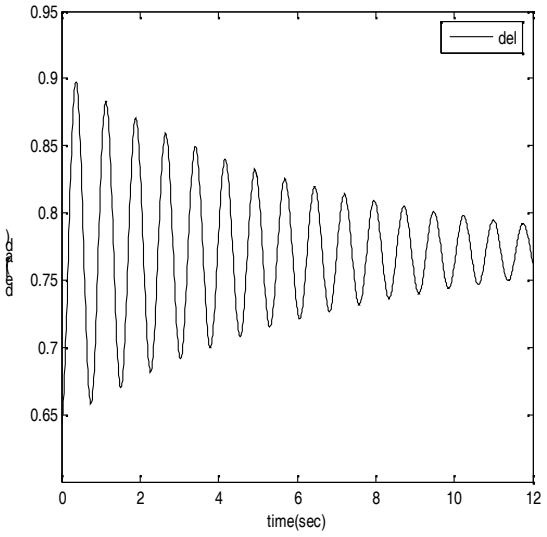

Figure 0.7: Plot of Generator angle without any external control signal applied

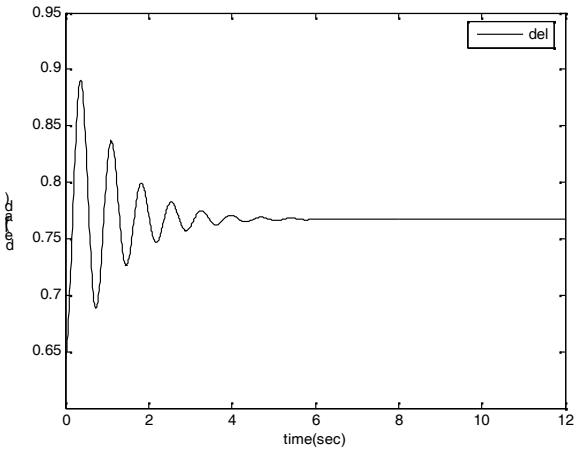

Figure 0.8: Plot of Generator angle with Δw as the auxiliary stabilizing signal (K_w= 1.4)

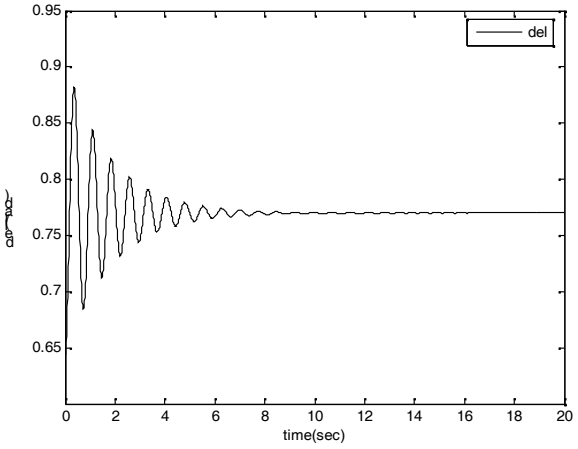

Figure 0.9: Plot of generator angle with ΔPac (change in power of adjacent AC line) as the auxiliary stabilizing signal (K_w= 0.1).

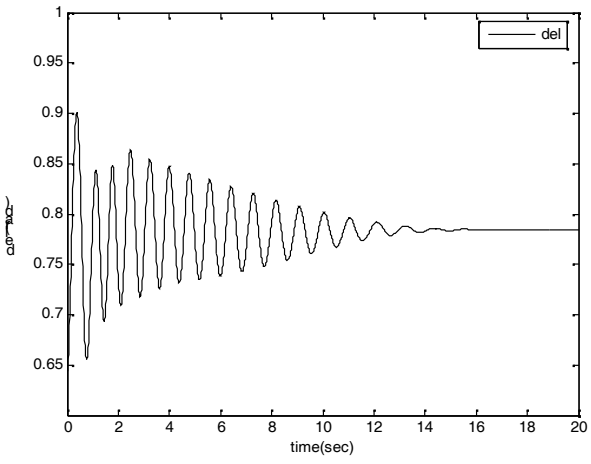

Figure 0.10: plot of generator angle with $\frac{d(\Delta\omega)}{dt}$ as the auxiliary stabilizing signal (K_d=0.45).

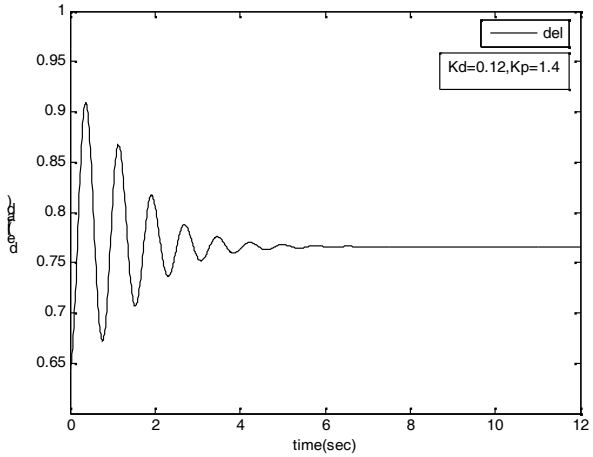

Figure 0.11: Plot of generator angle with K_p* Δw +K_d* $\frac{d(\Delta\omega)}{dt}$ as the auxiliary stabilizing signal (K_p=1.4, K_d =0.12).

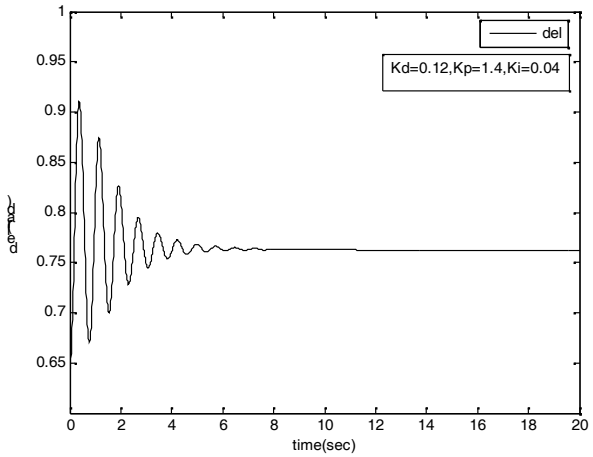

Figure 0.12: plot of generator angle with K_p* Δw +K_d* $\frac{d(\Delta\omega)}{dt}$ +K_iΔδ as the auxiliary stabilizing signal (K_p=1.4, K_d =0.12, K_i=0.04).

viii. Case B: Line Outage

One of the parallel AC lines is given outage, here the two ac lines are assumed to be similar. Therefore this disturbance can be reflected by varying the value of X_{eq}, which represents the equivalent reactance of both the lines. Here, once again the different signals are utilized for stability improvement. The plots of generator angles for different stabilizing signals are shown in figures 4.10 – 4.15.

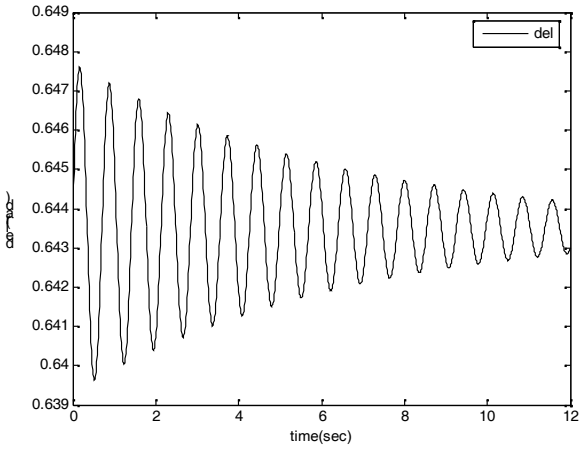

Figure 0.13: Plot of generator angle without any external control signal.

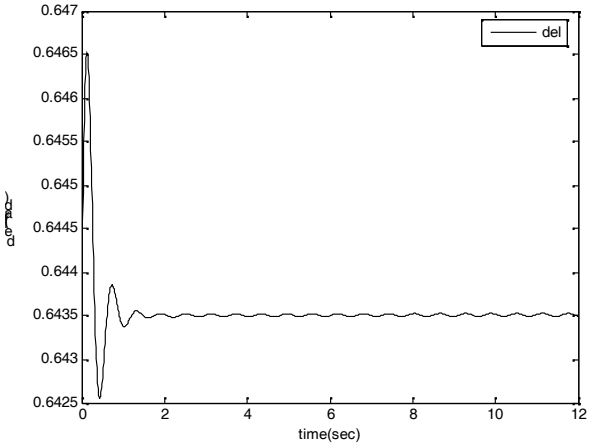

Figure 0.14: plot of generator angle with Δw as the auxiliary stabilizing signal (K_w=4.5).

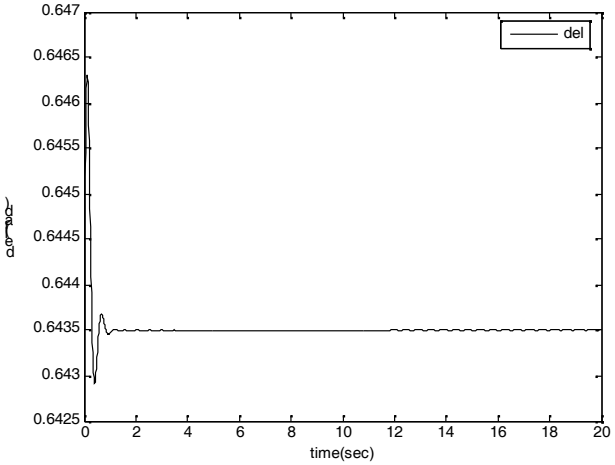

Figure 0.15: plot of generator angle with ΔPac (change in power of adjacent AC line) as the auxiliary stabilizing signal (K_w=2).

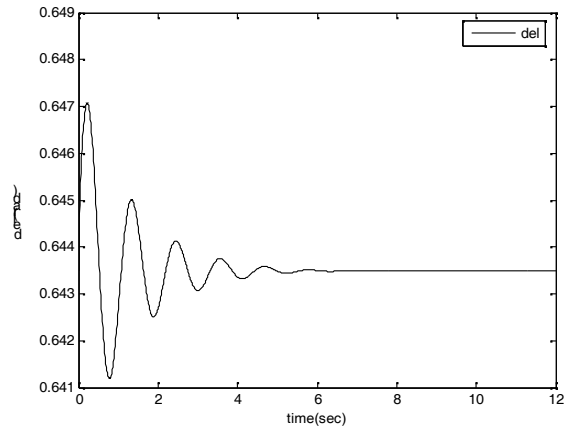

Figure 0.16: plot of generator angle with $\frac{d(\Delta\omega)}{dt}$ as the auxiliary stabilizing signal (Kd=1).

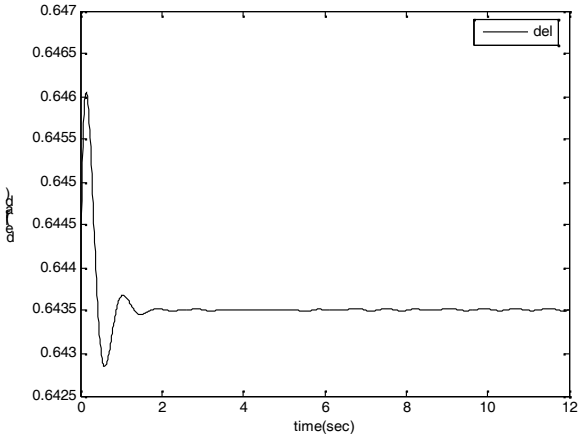

Figure 0.17: plot of generator angle with K_p* Δw +K_d* $\frac{d(\Delta\omega)}{dt}$ as the auxiliary stabilizing signal (K_p=4.5, K_d =0.5).

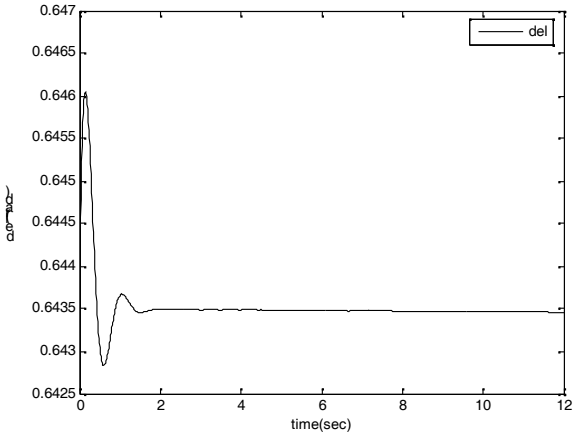

Figure 0.18: Plot of generator angle with K_p* Δw +K_d* $\frac{d(\Delta\omega)}{dt}$ +K_iΔδ as the auxiliary stabilizing signal (K_p=1.4, K_d =0.12, K_i=0.0005).

b. Multimachine System Analysis

The power flow through a HVDC link can be highly controllable. This fact is utilized to strengthen the power system stability. The WSCC – 9 Bus system is considered for the stability analysis and is given in the figure 4.16.

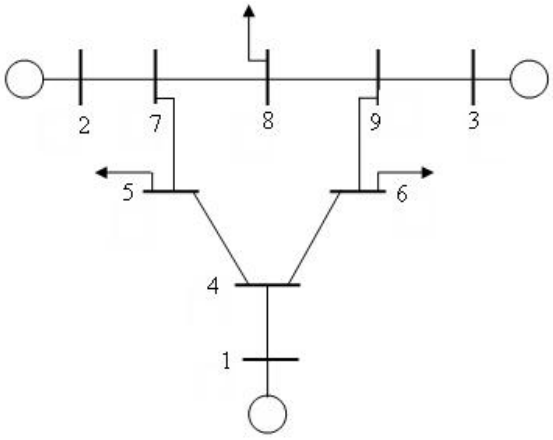

Figure 0.19: WSCC 9 Bus System

The scenario adapted for our study is given below:

A fault is assumed to occur on Line 4-6, at initial time zero. It is assumed that a grounded fault occurred near to Bus 6 and the line from Bus 4 to Bus 6 is removed after 4 cycles. The HVDC line is located between buses 4 –5. Under these conditions, the impact of HVDC on system stability is presented. Initially, a case in which the HVDC line maintains the same control as in the normal state, in which the post-fault HVDC power flow setting remains the same as before, is investigated. It was found that, the system becomes unstable. Then a PI controller is designed to stabilize the system. The controls are used to alter power flow setting in the HVDC line. The system data is given in appendix I.

i. Case I: Uncontrolled Case

Fig. 4.17 is a plot of the generator angles for a grounded fault at Bus 6. The HVDC line is in between buses 4 – 5. The post fault power flow setting through the HVDC line is the same as the pre-fault power flow setting. No extra control mechanism has been employed here. The plot of relative angles of the generator is shown in figure 4.18.

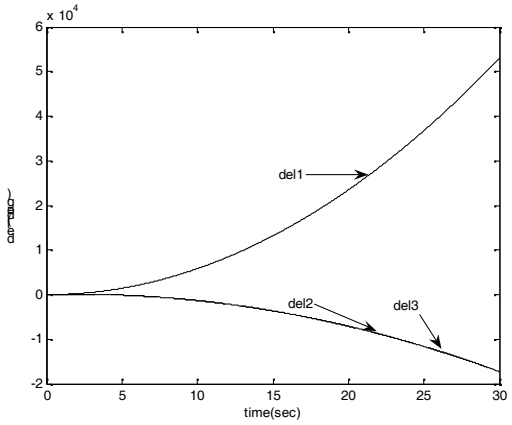

Figure 0.20: Plot of generator angles without any extra control

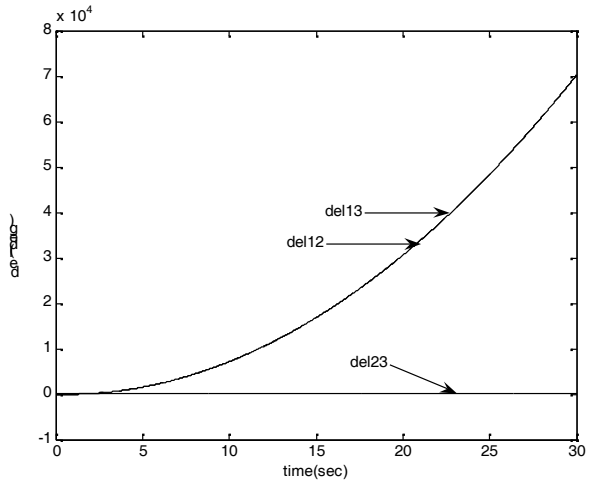

Figure 0.21: Plot of relative angles with no extra control

From Fig 4.17, it can be seen that angle of generator 1 goes unsynchronized from those of generators 2 & 3. In order to make the angle of generator 1, to be in step with those of the other two generator angles, the power mismatch at Bus 1 has to be altered. This can be achieved by changing the power flow in the HVDC line through an augmented feedback control.

When employing a feedback loop, the error signal is defined to average out the acceleration force for all the three machines as follows [9]:

$$e = \left[\frac{\frac{P\_mis(3)}{H(3)} + \frac{P\_mis(2)}{H(2)}}{2} \right] - \left[\frac{p\_mis(1)}{H(1)} \right] \quad (4.1)$$

where,

P_mis(i) = Real Power Mismatch at Bus 'i'

H(i) = Moment of Inertia of generator 'i'.

HVDC system's current controller and line dynamics are not considered in this analysis. Accordingly, a realistic simple model for HVDC is adopted in the stability calculations. The extra energy introduced by the fault will be eventually smoothed out by an AGC as long as the machines are kept synchronized.

ii. Case II: With PI Controller

System stability was augmented using a PI Controller. The control mechanism employed is given below [9]. Based on the error signal defined above, the flow in the DC line is changed as follows:

$$P_{di}^{k+1} = P_{di}^{k} - K_p e^k - K_i \int e(t)\,dt \quad (4.2)$$

where,

P_{di} = Active Power flow at the Inverter terminal.

K=Time step.

e= Error signal.

K_p=Proportional constant (=0.0013).

K_i= Integral constant (=0.00061).

Integral of error, I (t), is found out by trapezoidal method. The time interval [0, t] is divided into n time steps with an interval of Δt. Here k is the K^{th} time step, e_k=error at time step k and Δt= time step interval (=1/50). Accordingly,
for k = 1:n

$$I_k = I_{k-1} + \frac{1}{2}\left[e_k + e_{k-1}\right]\Delta t \quad (4.3)$$

With initial conditions, e_0 =0, I_0 = 0, and

$$I_k = \int_0^t e(t)\,dt \quad (4.4)$$

The plot of relative angles of the generators is as shown in figure 4.19 and the plot of generator phase angles is shown in figure 4.20.

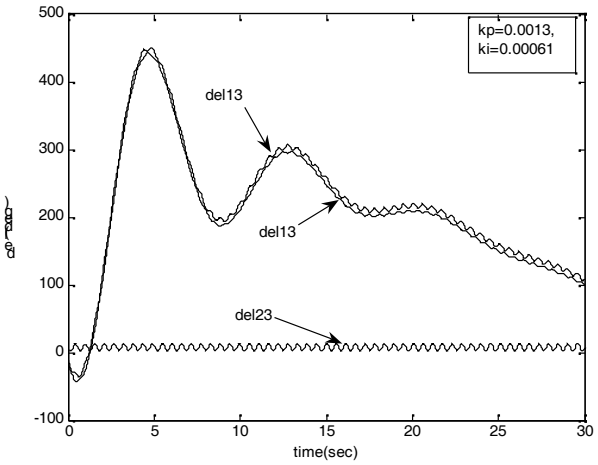

Figure 0.22: Plot of relative angles with PI control

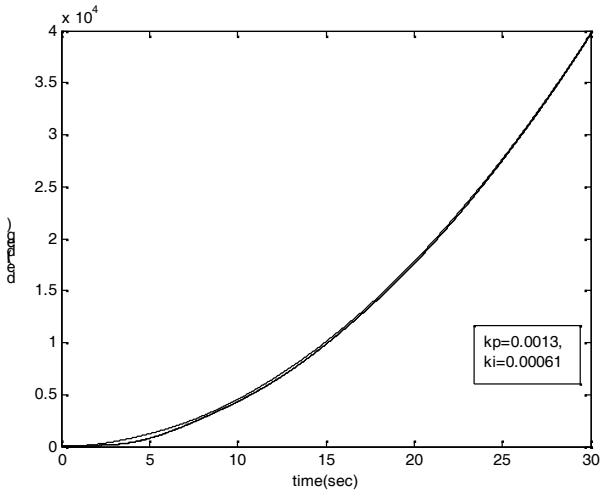

Figure 0.23: Plot of Generator angles with PI control

c.Multimachine System Considering Current Controller and Line Dynamics

Now considering the dynamics associated with the current controller and the DC line the stability study is performed again. The DC line is represented by the transfer function model.

i. Current Controller

Here, proportional integral current controller is used and is shown in figure 4.21

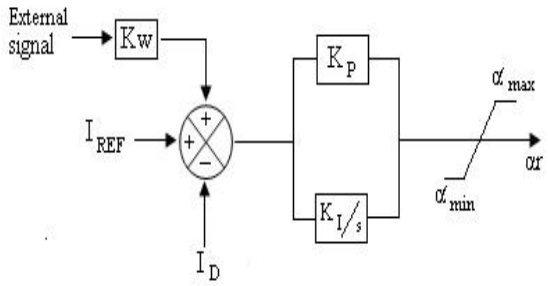

Figure 0.24: Current controller

ii. Auxiliary controller

Here, a simple constant gain Auxiliary controller is employed and is shown in figure 4.22. The stability of the system is improved by varying the gain constant (K_w) of the above controller.

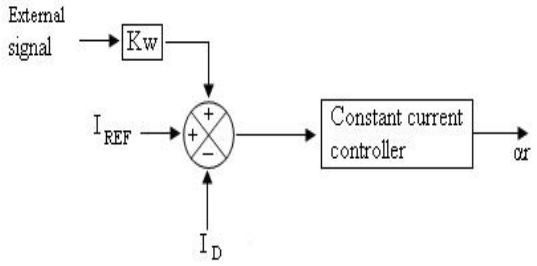

Figure 0.25: Constant Gain Controller

iii. Case 1 Uncontrolled case

Considering the same disturbance as in previous case, stability study is performed again. Here two extra differential equations representing the current controller and the HVDC Line dynamics are to be solved using the Runge – Kutta method. Here the taps are assumed to be constant and the mode shifts are not considered [1]. Without any extra control mechanism the plots of generator angles and their relative difference will be as shown in figure 4.23 and figure 4.24.

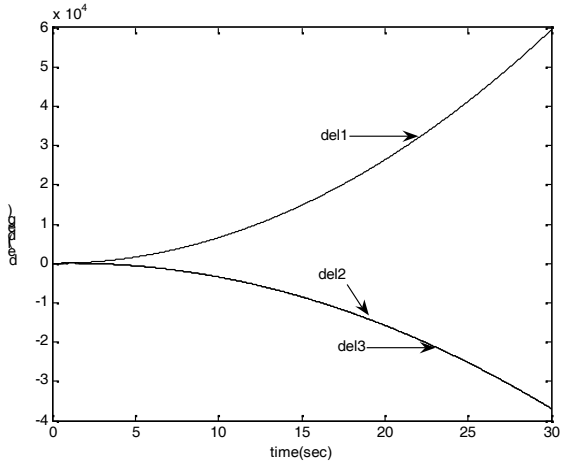

Figure 0.26: Plot of generator angles with no external control signal applied

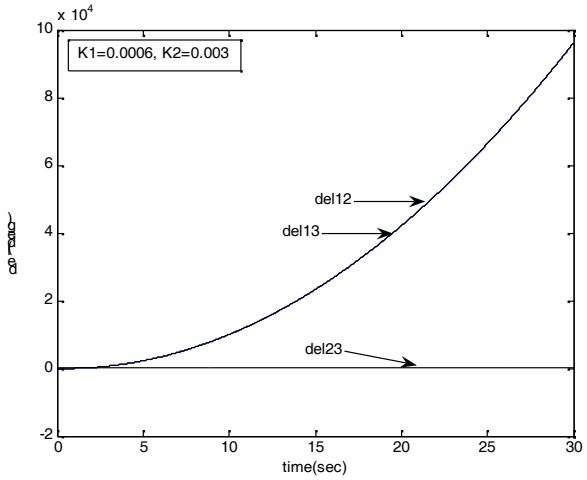

Figure 0.27: Plot of relative angles without any external control signal

It is clearly seen that the system is becoming unstable, generator 2 and generator 3 are moving together whereas generator 1 falling out of synchronism, with this group. Considering the following signals:

$$error_1 = \left[\left[\frac{(\omega(2)-\omega(1))+(\omega(3)-\omega(1))}{2}\right]-\left[\omega(2)-\omega(3)\right]\right] \quad (4.5)$$

$$error_2 = \left[\left[\frac{(del(2)-del(1))+(del(3)-del(1))}{2}\right]-\left[del(2)-del(3)\right]\right] \quad (4.6)$$

$$error_3 = \left[\frac{\frac{P\_mis(3)}{H(3)}+\frac{P\_mis(2)}{H(2)}}{2}\right]-\left[\frac{P\_mis(1)}{H(1)}\right] \quad (4.7)$$

The signal $error_1$, represents average error in the speed differences between the three generators. The signal error2, represents average error in relative angles between the three generators. The signal error3 is defined to average out the acceleration force for all the three machines. Different combinations of the above three signals are considered, in order to improve the stability.

iv. Case 2

Considering the signal $error_3$ as the control input, the plot of relative angles is as shown in the figure no 4.25.

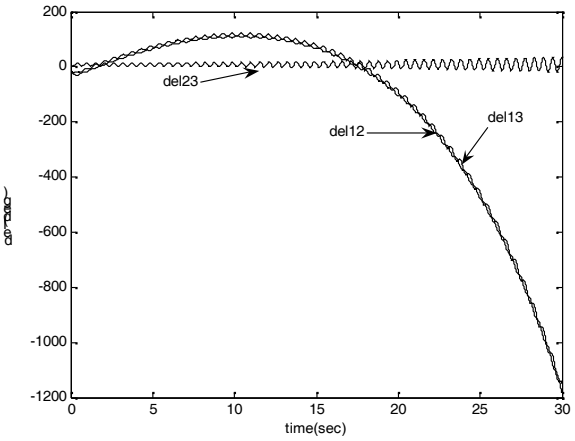

Figure 0.28:Plot of relative angles with $error_3$ as the control signal

v. Case 3

Considering the combination of $error_1$ and $error_2$ signals as the control input, the plot of relative angles is as shown in figure no 4.26.

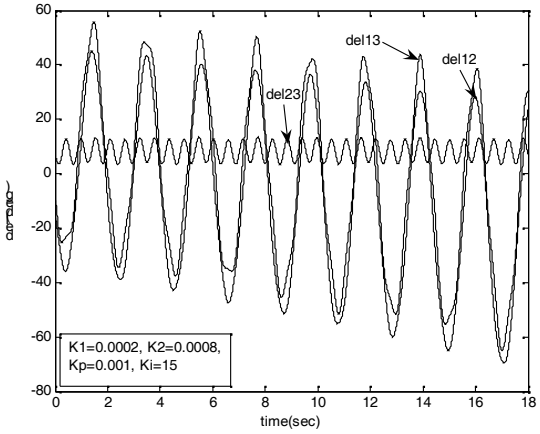

Figure 0.29: Plot of relative angles with $error_1$ and $error_2$ as control signals

vi. Case 4

Considering the combination of $error_1$ and $error_3$ signals to generate the required control signal, the plot of relative angles will be as shown in the figure no 4.27.

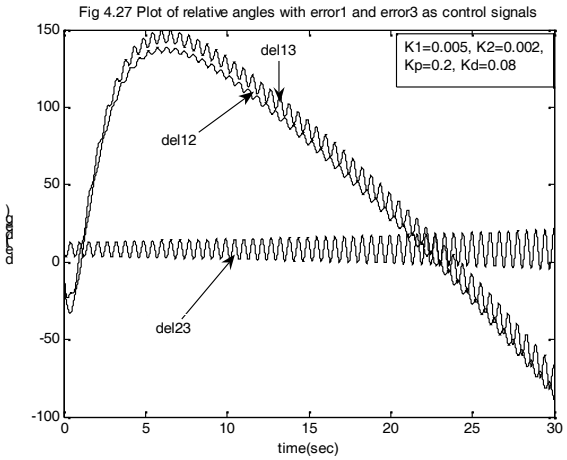

Figure 0.30: Plot of relative angles with $error_1$ and $error_3$ as control signals

vii. Case 5

Considering the combination of $error_2$ and $error_3$ signals to generate the control signals, the plot of relative angles will be as shown in figure no 4.28.

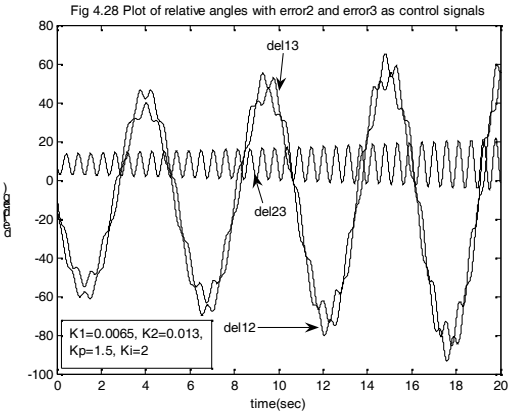

Figure 0.31: Plot of relative angles with $error_2$ and $error_3$ as control signals

viii. Case 6

Considering the combination of all the three signals to generate the control signal, the plots of the relative angles with different gains are as shown in figure (4.29) and figure (4.30).

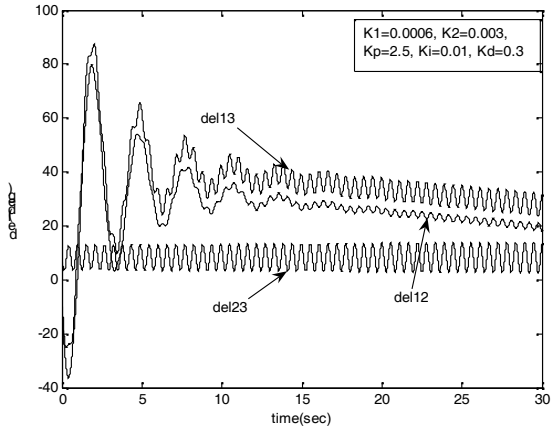

Figure no 0.32: Plot of relative angles with PID controller.

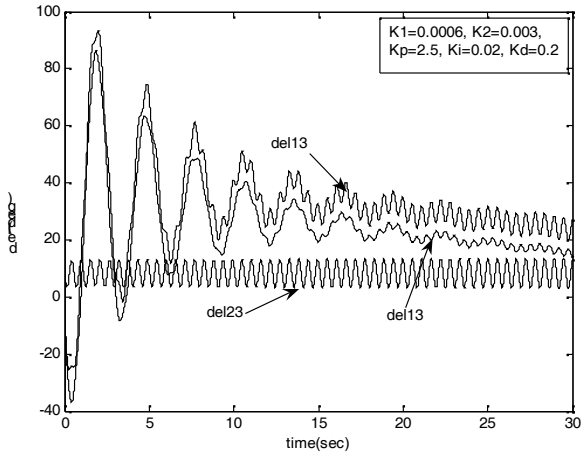

Figure 0.33: Plot of relative angles with PID controller

The study reveals that the system can be stabilized by using a controller which produces the control signal given in equation 4.8.

Control signal, error = K_p*$error_1$+ K_i*$error_2$ + K_d*$error_3$ (4.8)

Here the signal $error_2$ is the equivalent to the integral of the signal $error_1$, and the signal $error_3$ is equivalent to the differential of the signal $error_1$. Hence, the controller proposed above is equivalent to a PID controller. Then the control signal can be equivalently represented as in equation 4.9.

$$error= K_p\, e(t)+K_i\, Ie(t)+K_d\, De(t) \quad (4.9)$$

Considering this, the methodology used in variable gain PID controller scheme can be applied to the above controller, to improve its performance. In the next chapter, a Fuzzy PID controller scheme is proposed to improve the stability of the system.

V. CONCLUSIONS

For the variations in the mechanical power of the generator, in the single machine system, the speed change signal as a control signal is more effective as shown in figures 4.5 to 4.9. For a parallel line outage, the variation in power, in the other parallel line, when used as the control signal, gives better performance as shown in figures 4.10 to 4.15.

When the HVDC current controller and line dynamics are not considered, the transient stability of the multimachine system after the occurrence of the specified fault, is improved by using a PI controller with average acceleration as the control signal, as shown in figure 4.19

Considering the HVDC current controller and line dynamics, it is observed that the transient stability of the multimachine system is improved only if the combination of all the three signals derived from relative speed, phase angle and average acceleration are used, as shown in figures 4.23 to 4.30. This paper demonstrates that, control mechanisms can be designed and incorporated for HVDC power modulation, to augment the stability of the power system.

References

[1] P. Kundur, “Power System Stability and Control”, McGraw-Hill, Inc., 1994.

[2] Prabha Kundur, John Paserba, “Definition and Classification of Power System Stability”, IEEE Trans. on Power Systems., Vol. 19, No. 2, pp 1387- 1401, May 2004.

[3] A. Panosyan, B. R. Oswald, “Modified Newton- Raphson Load Flow Analysis for Integrated AC/DC Power Systems”,

[4] T. Smed, G. Anderson, “A New Approach to AC/DC Power Flow”, IEEE Trans. on Power Systems., Vol. 6, No. 3, pp 1238- 1244, Aug. 1991.

[5] Stagg and El- Abiad, “Computer Methods in Power System Analysis”, International Student Edition, McGraw- Hill, Book Company, 1968.

[6] Jos Arrillaga and Bruce Smith, “AC- DC Power System Analysis”, The Institution of Electrical Engineers, 1998.

[7] K. R. Padiyar, “HVDC Power Transmission Systems”, New Age International (P) Ltd., 2004.

[8] “IEEE Guide for Planning DC Links Terminating at AC Locations Having Low Short-Circuit Capacities”, The Institute of Electrical and Electronics Engineers, Inc., 1997.

[9] Garng M. Huang, Vikram Krishnaswamy, “HVDC Controls for Power System Stability”, IEEE Power Engineering Society, pp 597- 602, 2002.

[10] Choo Min Lim, Takashi Hiyama, “Application of A Rule-Based Control Scheme for Stability Enhancement of Power Systems”, pp 1347- 1357, IEEE 1995.

P. Bapaiah received Diploma in Electrical and Electronics Engineering from A.A.N.M&V.V.R.S.R Polytechnic, Gudlavalleru (INDIA) in 2002**.** Received his Bachelor degree in Electrical and Electronics Engineering from Gudlavalleru Engineering College, Gudlavalleru (INDIA) in 2006.Worked as Site Engineer in MICRON Electricals at Hyderabad in 2006-2008. And M.Tech in Power Systems Engineering from V.R.Siddhartha Engineering College, Vijayawada, Acharya Nagarjuna University Guntur, (INDIA) in 2010. He is currently working as an Assistant Professor in Electrical and Electronics Engineering Department at Amrita Sai Institute of Science and Technology, Paritala, (INDIA). His research interests include Power Systems, HVDC Transmission Systems, and Power Quality.